Nonperturbative Quantum Electrodynamics in the Cherenkov Effect

Charles Roques-Carmes,[1,*] Nicholas Rivera,[2] John D. Joannopoulos,[2] Marin Soljačić,[1,2] and Ido Kaminer[3,†]

[1]*Research Laboratory of Electronics, Massachusetts Institute of Technology,
Cambridge, Massachusetts 02139, USA*
[2]*Department of Physics, Massachusetts Institute of Technology, Cambridge, Massachusetts 02139, USA*
[3]*Department of Electrical Engineering, Technion-Israel Institute of Technology, Haifa 32000, Israel*

Quantum electrodynamics (QED) is one of the most precisely tested theories in the history of science, giving accurate predictions to a wide range of experimental observations. Recent experimental advances allow for the ability to probe physics on extremely short attosecond timescales, enabling ultrafast imaging of quantum dynamics. It is of great interest to extend our understanding of short-time quantum dynamics to QED, where the focus is typically on long-time observables such as S matrices, decay rates, and cross sections. That said, solving the short-time dynamics of the QED Hamiltonian can lead to divergences, making it unclear how to arrive at physical predictions. We present an approach to regularize QED at short times and apply it to the problem of free-electron radiation into a medium, known as Cherenkov radiation. Our regularization method, which can be extended to other QED processes, is performed by subtracting the self-energy in free space from the self-energy calculated in the medium. Surprisingly, we find a number of previously unknown phenomena yielding corrections to the conventional Cherenkov effect that could be observed in current experiments. Specifically, the Cherenkov velocity threshold increases relative to the famous conventional theory. This modification to the conventional theory, which can be non-negligible in realistic scenarios, should result in the suppression of spontaneous emission in readily available experiments. Finally, we reveal a bifurcation process creating radiation into new Cherenkov angles, occurring in the strong-coupling regime, which would be realizable by considering the radiation dynamics of highly charged ions. Our results shed light on QED phenomena at short times and reveal surprising new physics in the Cherenkov effect.

DOI: 10.1103/PhysRevX.8.041013   Subject Areas: Optics, Photonics, Quantum Physics

I. INTRODUCTION

One of the early achievements of quantum electrodynamics (QED) was the accurate match of the predicted hydrogen-energy-level shifts with the experiments by Lamb and Retherford [1]. This significant accomplishment was allowed by the work of Tomonaga [2], Bethe [3], Schwinger [4], and Feynman [5] and the later unification by Dyson [6]. They eliminated the problematic divergence of the Lamb-Retherford shift due to the photon loop correction to the atom's propagator. Renormalization of the electron mass also led to a very precise agreement with the experimentally measured values of the Lamb-Retherford line shift [1], the anomalous magnetic moment of the electron [7], and the anomalous hyperfine splitting of the ground state of the hydrogen atom [8]. Since these early

successes, QED has been one of the most accurate theories of modern physics and bolstered fundamental developments, from quantum field theory to grand unified theories. Central to calculations in QED and other field theories is the S matrix, representing the long-time transition amplitude between an initial state and some final state [9–11]. From the S matrices, one can derive many important observables such as decay rates, cross sections, and self-energies, which have been successfully used to calculate a great variety of effects in particle physics, condensed matter physics, atomic physics, and many other fields. Despite these successes, S-matrix methods are essentially used to make predictions at infinite times. Altogether in QED, very few studies consider the physics at short times (e.g., Refs. [12–14]) and almost none when considering the coupling to a continuum of electromagnetic modes. We still lack the basic methods to describe the short-time dynamics in such systems, where it remained unknown how to apply renormalization at finite times.

One of the emblematic problems in light-matter interaction that can be used as a testing ground for new ideas in QED is the Vavilov-Cherenkov effect (abbreviated as the Cherenkov effect)—the radiation by a charged particle propagating in a dispersive medium at a speed larger than

*[*]chrc@mit.edu
[†]kaminer@technion.ac.il

the phase velocity of light in the medium. It is the leading-order process in the radiation by a free electron in a medium and is the fundamental building block for any diagram describing the interaction of charges with photons in a medium. This effect was originally observed by Vavilov and Cherenkov in 1934 [15,16] and later explained by Frank and Tamm [17]. Most of the quantum treatment of this problem, which originated from Ginzburg's Ph.D. thesis [18], did not result in a significant deviation from the original prediction by Frank and Tamm [17]. Even later theories taking into account higher-order processes did not find regimes where the quantum nature of the interacting particles would result in a significant mismatch from the original prediction of Frank and Tamm [17–19]. Only recently was it theoretically predicted that quantum effects could emerge in the optical regime when taking into account the quantum recoil of the electron or shaping the electron wave function [20].

Despite the many years that have passed since the original discovery of the Cherenkov effect, it continues to lead to new discoveries in different systems including heavy-ion jets [21–26], nonlinear phase-matched systems [27–33], moving vortices in Josephson junctions [34,35], condensed-matter analogue models of gravitational physics, and moving dipoles showing the hybridization of the Cherenkov and Doppler effects [36–38]. The concept of the Cherenkov velocity threshold is also found in the theory of superfluidity and Landau damping of highly confined plasmons [39,40], two topics of major interest these days. New physics in the Cherenkov effect, such as backward Cherenkov radiation [41], was unveiled with free electrons propagating in complex nanophotonic systems: photonic crystals [42], metamaterials [43–45], plasmonic systems [46], and graphene [47]. This continued interest in explaining the theory of Cherenkov radiation in novel settings originates in its wide range of applications, from high-energy particle characterization [48] to biomedical imaging [49].

The Cherenkov effect follows the Frank-Tamm formula that gives the rate of photon emission per unit frequency $\partial_\varepsilon \Gamma_{\mathrm{rad}} = [(\alpha_Z \beta)/\hbar]\{1 - [1/(n_\varepsilon \beta)^2]\}$. In this expression, $\alpha_Z = Z^2 \alpha$ is the effective fine-structure constant, $\alpha \approx 1/137$ being the fine-structure constant and Z the particle charge; $\beta = v/c$, v being the electron speed and n_ε the refractive index of the medium (function of the photon energy $\varepsilon = \hbar\omega$). From the Frank-Tamm formula and its generalizations to nanostructured optical systems or anomalous cases [42,50], one sees that, in the optical regime, the timescale at which a photon is emitted in the medium is between picoseconds and femtoseconds. Physics at these timescales was unveiled at the turn of the millennium with the development of ultrafast optics, light-wave electronics, and high harmonic generation [51]. Today, the integration of electron optics with optical technologies allows the probing of atomic transitions [51], molecular bonding [52], and even more recently

dynamics of plasmonic systems [53–59]. Given these new experimental techniques, it is timely to ask how the long-standing physics of the Cherenkov effect changes at very short timescales.

In this article, we develop a general framework for time-dependent QED, which is free of short-time divergences, and use our framework to reveal new underlying phenomena in Cherenkov radiation. This process yields concrete closed-form solutions of the power spectrum of photon emission and a surprising increase in the Cherenkov velocity threshold. Applying our theory to probe the time dependence of the emitted radiation from a charged particle propagating in a medium, we observe new quantum phenomena in the Cherenkov effect. Even when the electron and photon are weakly coupled ($\alpha \ll 1$), the well-known Cherenkov dispersion relation is modified from the known one on account of a nonzero self-energy associated with the virtual emission and reabsorption of photons in the medium. When pushing the limits of our formalism to strongly coupled regimes ($\alpha Z^2 \gtrsim 1$), we find evidence of regimes where the electron experiences a nonexponential decay and the Cherenkov dispersion relation changes drastically. In these strongly coupled settings, we predict the emergence of multiple Cherenkov lines that can be tested in existing experiments such as heavy-ion colliders. More generally, the Cherenkov effect provides us with a powerful playground to develop new general tools for time-dependent QED. Our work suggests applications in the study of fundamental effects in attosecond physics, such as high harmonic generation, and new experimental endeavors of Cherenkov radiation and its analogues in strongly coupled settings.

II. TIME-DEPENDENT NONPERTURBATIVE THEORY OF CHERENKOV RADIATION

We consider the system shown in Fig. 1. A charged particle, such as a single electron or a highly charged ion, is propagating at speed $v = \beta c$ inside a lossless material defined by its refractive index n_ε. According to the conventional Cherenkov theory, if the particle velocity surpasses the speed of light in the medium $\beta > c/n_\varepsilon$, it emits a photon of energy ε at angle θ_C relative to the electron trajectory, satisfying the condition [Fig. 1(a)] $\cos\theta_C = [1/(n_\varepsilon\beta)]$ [17]. This energy-angle relation is a direct consequence of energy-momentum conservation [60], while the photon emission rate per unit energy can be derived from Fermi's golden rule [18].

We solve for the time dependence of the time-evolution operator corresponding to the QED Hamiltonian using the resolvent method [10]. This method allows us to perform resummations of partial sets of the perturbation series in a compact algebraic formulation while maintaining dynamical information of the correlated electron-photon wave function. The method works as follows: We reformulate the Schrödinger equation in terms of the resolvent

Conventional Cherenkov   **Quantum corrected Cherenkov**

(a)   (b)   Weak-coupling regime   (c)   Strong-coupling regime

$$\Gamma_{\rm rad} = \frac{\alpha\beta}{\hbar} \int d\varepsilon \left(1 - \left(\frac{1}{n_\varepsilon\beta}\right)^2\right) \qquad\qquad \bar{\Gamma}_{\rm rad} = \frac{\alpha\beta}{\hbar} \int d\varepsilon \left(1 - \left(\frac{\varepsilon - z_0}{\varepsilon n_\varepsilon\beta}\right)^2\right)$$
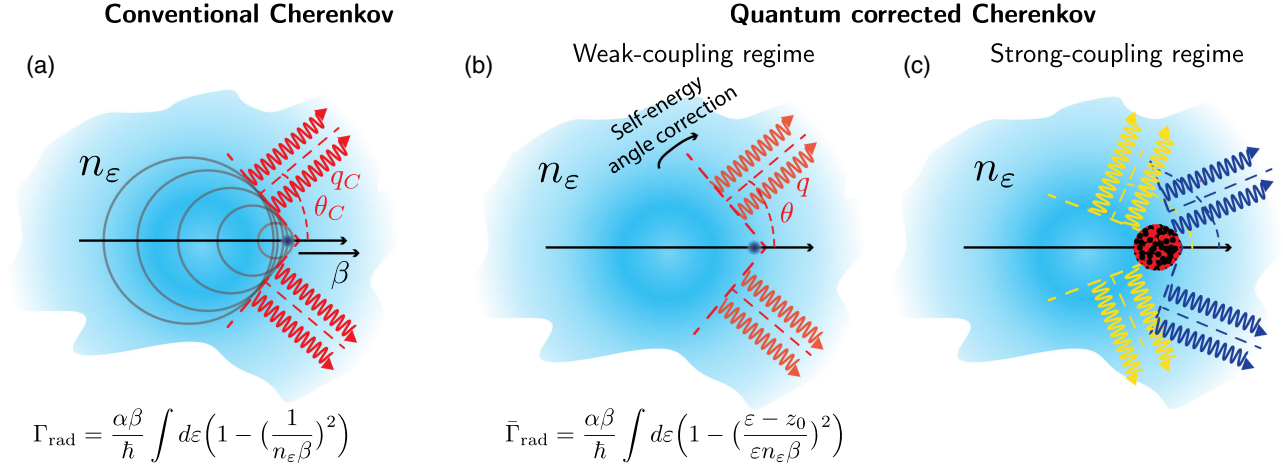
FIG. 1.   The quantum Cherenkov effect. (a) Conventional Cherenkov effect. (b) Regularized quantum Cherenkov effect for an electron (weak coupling), where the particle's regularized self-energy is a small correction. (c) Regularized quantum Cherenkov effect for a highly charged ion, where the self-energy results in large corrections.

operator $G(z) = (z - H)^{-1}$, which is the complex-variable Fourier transform of the unitary time-evolution operator, used to determine the time-dependent electron-photon wave function. The matrix elements of G represent the Fourier transform of transition amplitudes between different states. We first derive a matrix equation for $G_0 \equiv \langle p, 0|G|p, 0 \rangle$ (for more details on the formalism and the QED Hamiltonian, we refer to Appendix A). Inverting the matrix equation and moving back into the time domain, we find the following expressions for the evolution operator projected on the zero-photon state $U_0(t)$ and the probability of observing a photon $p_1(t)$:

$$U_0(t) = \frac{1}{\pi} e^{-iE_i t/\hbar} \int_{\mathbb{R}} dz\, e^{-izt/\hbar} \frac{\frac{\Gamma(z)}{2}}{[z - \Delta(z)]^2 + (\frac{\Gamma(z)}{2})^2}, \quad (1)$$

$$p_1(t) = \frac{1}{\hbar^2} \int dz \frac{\Gamma(z)}{2} \left| \int_0^t dt' e^{-izt'/\hbar} e^{iE_i t'/\hbar} U_0(t') \right|^2, \quad (2)$$

where E_i (respectively, E_f) is the charged particle's initial (final) energy and $p_0 = |U_0|^2$ the probability of the electron being in a state with zero photons. Equation (1) can be seen as a modification of the exponential decay law. In particular, when $\Delta(z)$ and $\Gamma(z)$ are constant, this corresponds to the usual exponential decay law for spontaneous emission which is valid at intermediate times. Similar modifications have been studied in the case of two-level systems [10] and for quasistationary states [61]. From Eqs. (1) and (2), one can derive time-dependent physical observables such as the spectrum of emitted photons per unit angle and per unit frequency $\partial^2 p_1/\partial\varepsilon\partial u$, which can also be used to determine the rate of photon emission. Figure 2 shows several examples of such spectral emission rates. In Eq. (1), $\Delta(z)$ and $\Gamma(z)$, which fully specify the dynamics of the system, are the real and imaginary parts, respectively, of the self-energy of the

electron $f(z)$ [also known as the radiative shift in atomic, molecular, and optical (AMO) physics]:

$$f(z + i0^{\mp}) = \frac{\alpha_Z \beta^2}{2\pi} \int_0^\infty d\varepsilon \int_{-1}^1 du \frac{n_\varepsilon \varepsilon (1 - u^2)}{z + i0^{\mp} - \varepsilon(1 - n_\varepsilon\beta u)}$$

$$:= \Delta(z) \pm i \frac{\Gamma(z)}{2}. \quad (3)$$

The real and imaginary parts of the self-energy function can be written analytically as

$$\Delta(z) = \frac{\alpha_Z \beta}{2\pi} \int_0^\infty d\varepsilon \left(\frac{2(z - \varepsilon)}{n_\varepsilon \varepsilon \beta}\right)$$

$$+ \left[1 - \left(\frac{z - \varepsilon}{n_\varepsilon \varepsilon \beta}\right)^2\right] \log\left|\frac{z + \varepsilon[n_\varepsilon\beta - 1]}{z - \varepsilon[n_\varepsilon\beta + 1]}\right|, \quad (4)$$

$$\frac{\Gamma(z)}{2} = \frac{\alpha_Z \beta}{2} \int_0^\infty d\varepsilon \left[1 - \left(\frac{\varepsilon - z}{\varepsilon n_\varepsilon\beta}\right)^2\right] \Theta\left[\left(\frac{\varepsilon - z}{\varepsilon n_\varepsilon\beta}\right)^2 \leq 1\right], \quad (5)$$

respectively, where $\Theta[.] = 1$ if the condition between brackets is satisfied, $\Theta[.] = 0$ otherwise.

$\Delta(0)$ and $\Gamma(0)$ exactly match the real and imaginary part, respectively, of the radiative shift calculated via the second-order perturbation theory in the weak-coupling regime. More generally, $\Delta(z)$ and $\Gamma(z)$ correspond to the second-order perturbation of the energy, shifted by the complex frequency variable z. Our approach is nonperturbative in the sense that the self-energy function models absorption and reemission cycles of the photon before a final photon emission, thus taking into account an infinite sum of single-loop Feynman diagrams (see Fig. S4 in Supplemental Material [62]). We add additional diagrams altering the electron after the photon emission, showing quantitative corrections but no qualitative changes to our predictions (see Ref. [62], Sec. I). Our theory could be extended to take
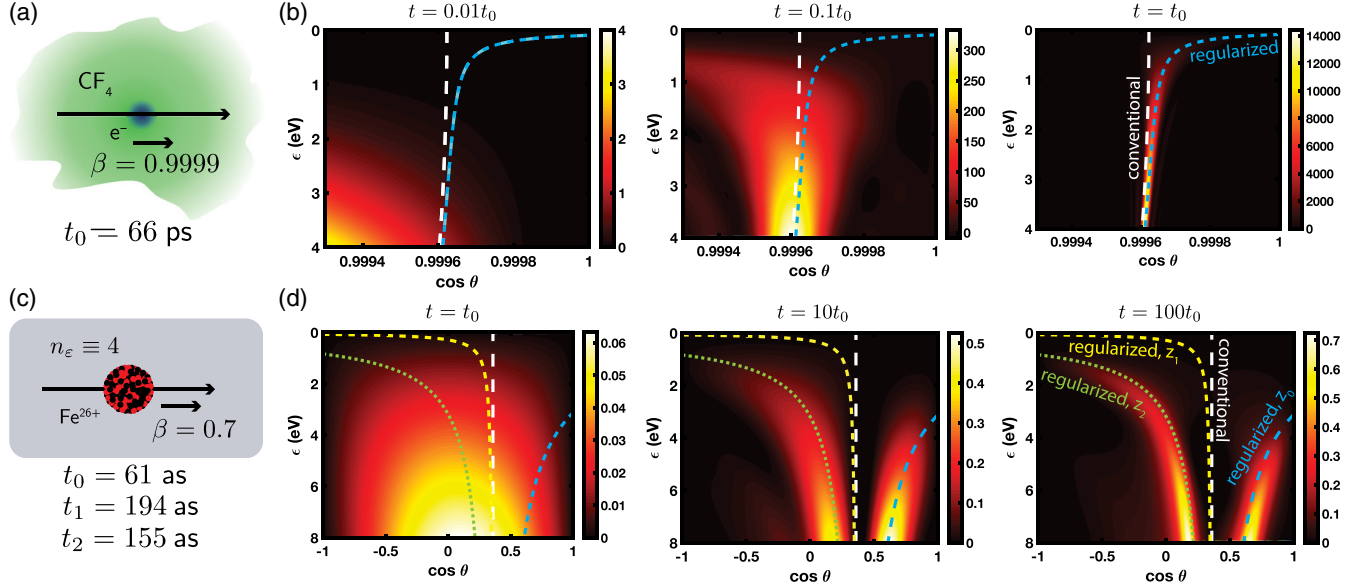
FIG. 2. Nonperturbative self-energy-induced modifications to Cherenkov radiation in weakly and strongly coupled regimes. (a) [respectively, (c)] An electron propagating at velocity $\beta = 0.9999$ (respectively, $\beta = 0.7$) in a chamber filled with CF_4 gas (respectively, in a material of constant index equal to 4) emits a photon with spectral angular density $[(\partial^2 p_1)/(\partial \varepsilon \partial u)](t)$, where $u = \cos\theta$ shown in (b) [respectively, (d)] at different times. The gradual narrowing of the Cherenkov energy-angle relation for long times is a direct consequence of the time-energy uncertainty principle.

into account higher-order processes with a more sophisticated numerical treatment [63].

III. THE RADIATIVE SHIFT OF THE FREE ELECTRON

Upon a first evaluation of the self-energy, we find that the real part features a UV divergence as a result of the unbounded photonic density of states at high energies [64], even when the index of refraction is too low for Cherenkov radiation. Nevertheless, we regularize the self-energy function in a way that agrees with physical predictions, by subtracting its free-space part ($n_\varepsilon \equiv 1$):

$$f(z) \rightarrow f(z) - f(z, n_\varepsilon \equiv 1). \qquad (6)$$

To get the conservation of probability, we substitute the regularized form of $\Gamma(z)$ in Eq. (2), which yields $p_0(t) + p_1(t) \equiv 1$. Regularizing the spectral angular density of the emitted photon also suppresses unphysical emission in free space (see Appendix B and Ref. [62], Sec. I, for further discussion of this point). This approach could be extended to any optical medium, as it takes into account material dispersion, and can be directly generalized to arbitrary geometries of photonic structures, by taking into account the eigenmodes of Maxwell's equations for such structures. Thus, our approach can be used in a wide range of phenomena stemming from the Cherenkov effect, including Cherenkov variants in 2D materials [47,65], in circuit QED [34,35], and in heavy-ion physics [22]. Moreover, this regularization approach can

be extended to other types of electron-photon interactions. For example, we propose a regularization scheme to give well-defined time dynamics for electron-photon (Compton) scattering in vacuum in Ref. [62], Sec. III.

When the coupling to light is weak—as in the case of an electron moving through a typical optical medium—we find that the contribution of the self-energy function in Eqs. (1) and (2) can be approximated by its value taken at the zero of $\Delta(z) - z$, which we denote as $z_0 = \Delta(z_0)$. This approximation, known as the flat-continuum approximation, retains validity when the decay rate or linewidth of the electron-emission process associated with Cherenkov radiation is much narrower than the frequency variation of the photonic density of states.

We find that the real part of the self-energy—known as the radiative shift z_0 [10]—is typically of the order of $-\alpha\beta^2/(2\pi)\Delta\varepsilon \sim -0.001$ eV for a single electron in the optical regime [see Appendix C, Eq. (C12)]. This free-electron radiative shift is significantly greater than its atomic counterpart—the Lamb-Retherford shift [1]—and, as a result, leads to potentially large corrections to quantum observables for small photon energies or particle velocities close to the conventional Cherenkov threshold ($n_\varepsilon\beta \rightarrow 1$). In particular, it modifies the well-established Cherenkov rate of emission to become

$$\partial_\varepsilon \bar{\Gamma}_{\text{rad}} = \frac{\alpha_Z \beta}{\hbar} \left[1 - \left(\frac{\varepsilon - z_0}{\varepsilon n_\varepsilon \beta} \right)^2 \right]. \qquad (7)$$

(We denote with a bar sign every quantum observable and state probability from our *regularized* theory—taking into

account the particle-regularized self-energy—in contrast to the conventional Cherenkov theory.) Additional corrections can come up from our quantum formalism. They typically include the electron recoil due to the Cherenkov emission of a single photon [20,47], which depends on the photon momentum $n_\varepsilon \varepsilon/c$ relative to the electron momentum $\beta E_i/c$. The radiation-angle correction is proportional to the radiative shift z_0 and to the electron recoil. In scenarios where the electron recoil is large [47], we expect to observe additional large self-energy corrections. Even without electron recoil, the radiative shift z_0 still significantly modifies the Cherenkov decay rate. This modification makes the new quantum corrections that we find far bigger than any previously found quantum effects in Cherenkov radiation [18,20].

Figure 3 shows that the account of the nonperturbative self-energy can shift the well-known Cherenkov threshold: $1/(n_\varepsilon \beta) \leq \varepsilon/(\varepsilon - z_0) \approx 1 + z_0/\varepsilon$ for small negative values of z_0. As a consequence, the regularized rate of emission $\partial_\varepsilon \bar{\Gamma}_{rad}$ converges to zero when approaching the regularized

Cherenkov threshold: In an experiment, this convergence translates into arbitrarily fewer photons emitted, compared to the conventional prediction. The most extreme deviation is found when the particle velocity is above the conventional threshold and below the regularized threshold, where the conventional theory predicts a finite rate of emission, while the regularized theory states that the spontaneous emission of a photon is forbidden.

Far above the conventional Cherenkov velocity threshold, the values of the regularized decay rate $\Gamma(z_0) = \Gamma_0$ and of the conventional decay rate $\Gamma(z = 0)$ agree, as can be seen in Fig. 3(b). However, the divergence of $1/\Gamma_0$ around $\beta \gtrsim \bar{\beta}_{th}$ results in arbitrarily small decay rates that directly translate on the dynamics of $p_0(t)$, as illustrated in Fig. 4(a). While the conventional theory predicts a total absence of decay below the conventional Cherenkov threshold, the regularized probability of the zero-photon state decays to a value of $1/\{1 - [d\Delta(z)/dz]|_{z_0}\}^2$ slightly below unity [Fig. 3(b)]. This result could be interpreted as the electron transitioning to a modified ground state of its energy dressed by the Cherenkov coupling, or it may
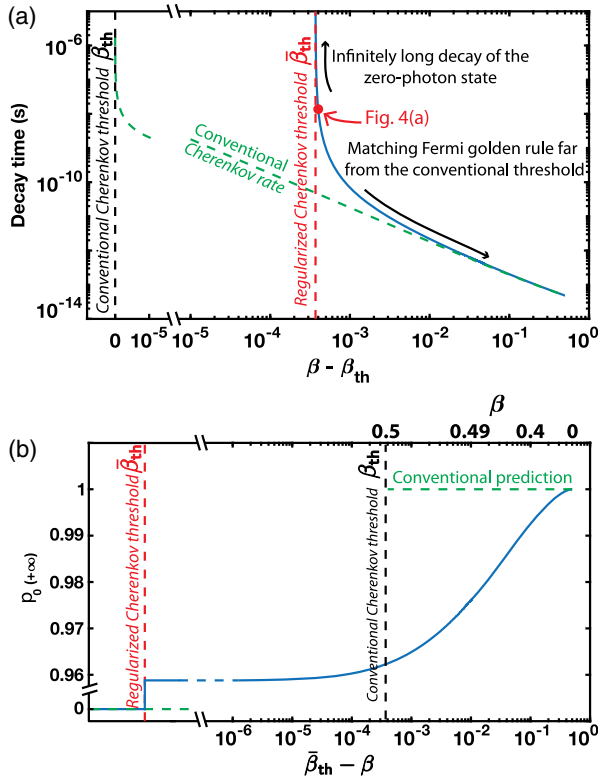

FIG. 3. The modified Cherenkov velocity threshold. (a) Regularized decay rate (blue curve) as a function of the distance to the conventional Cherenkov threshold β_{th}, above this threshold. (b) Probability of no Cherenkov emission $p_0(+\infty)$ as a function of the distance to the conventional Cherenkov threshold $\bar{\beta}_{th}$, below this threshold. The system considered for this example is a single electron traversing an index window defined by $n_\varepsilon = 2 * \mathbb{1}(\varepsilon \in [0, 5 \text{ eV}])$ [where $\mathbb{1}(\varepsilon \in A)$ is the indicator function of a subset of energies A]; however, similar effects occur regardless of the choice of particle or transparent index medium.
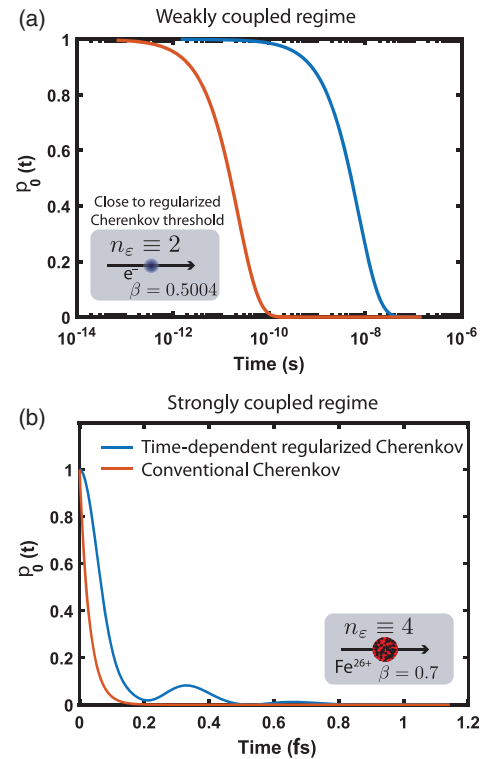

FIG. 4. Modified time dynamics in weakly and strongly coupled regimes. (a) Comparison of the regularized and conventional evolution of $p_0(t)$ for an electron very close to the regularized Cherenkov threshold $\beta - \bar{\beta}_{th} \approx 3 \times 10^{-5}$. Here, an electron propagating at a speed of $\beta = 0.5004$ emits a photon (e.g., its zero-photon state probability decays) at a rate that is 2 orders of magnitude less than the conventional prediction. (b) In strongly coupled regimes, the presence of several poles of the function $f(z)$ can result in a pseudoperiodic decay of $p_0(t)$.

complete a full decay when introducing higher-order diagrams including additional, multiple, photons. Far below the conventional Cherenkov threshold, the behaviors of the conventional and regularized theories match again. We observe a discontinuous transition in the behavior above and below the Cherenkov velocity threshold, which is essentially due to a discontinuous derivative of $\Gamma(z)$. However, we expect higher-order processes, that are neglected in the current formalism, to smoothen this transition: For multiphoton emission processes, the phase space for emission is larger, allowing for the emission of photons that do not individually satisfy the conventional Cherenkov relation.

This modification of the Cherenkov threshold has direct implications on the time-dependent spectrum of Cherenkov radiation, compared to the conventional theory. Our theory reveals ultrafast dynamics of Cherenkov radiation, for which we already observe significant modifications to the well-known observables: its energy-angle relation and the corresponding photon rate of emission. Specifically, Fig. 2(b) shows the implications of the time-energy uncertainty principle broadening the Cherenkov dispersion at very short times. These new effects can be seen through the flat-continuum approximation [10], where the radiative shift z_0 results in an effective decay rate that we denote as $\Gamma_0 = \Gamma(z_0)$. This approximation can be applied to Eq. (1), as it resembles the Fourier transform of a Lorentzian peaked at $z = z_0$. The Fourier transform yields an exponential decay with the rate $\Gamma_0/\hbar$: $U_0(t) \approx e^{-i(E_i+z_0)t/\hbar} e^{-\Gamma_0 t/2\hbar}$ $[p_0(t) \approx e^{-\Gamma_0 t/\hbar}]$ with $\partial^2 p_1(t)/\partial\varepsilon\partial u$ peaked around $E_f - E_i = z_0$, corresponding to the regularized Cherenkov dispersion relation shown in Fig. 1(b), with a finite width in the angular domain proportional to Γ_0 [Fig. 2(b)]. However, our predictions remain qualitatively valid only for times comparable to or less than the effective decay time of the zero-photon state $\hbar/\Gamma_0$, after which it is no longer legitimate to assume a single photon is emitted. To account for longer times, it is necessary to extend the dimension of the initial Hilbert space, allowing the emission of more than a single photon (such an approach is proposed and discussed in Ref. [62], Sec. I). For dynamics at short timescales of the Cherenkov effect, which are of primary interest, this restriction is unimportant, and our theory remains predictive.

IV. BIFURCATION BETWEEN WEAKLY AND STRONGLY COUPLED REGIMES

Intriguing consequences of our nonperturbative formalism arise when pushing the limits of our formalism to the strong-coupling regime in which the effective fine-structure constant significantly increases, $\alpha_Z = Z^2\alpha \gtrsim 1$, leading to the collapse of the flat-continuum approximation, which was accurately describing the physics above but does not hold here. Note that while in typical quantum field theories

the coupling constants scale like αZ, the coupling relevant to the Cherenkov effect actually scales like αZ^2, because it is an effect of a single vertex diagram. Physically, the strong coupling could be realized in the Cherenkov dynamics of highly charged ions. In the strongly coupled case, we find that multiple zeros, z_i, of $\Delta(z_i) - z_i = 0$ exist, allowing for a multibranched Cherenkov dispersion relation, with multiple Cherenkov angles θ_i satisfying $\cos\theta_i = [(\epsilon - z_i)/(n_\epsilon\epsilon\beta)]$ for multiple z_i, as illustrated in Fig. 1(c). In Fig. 2(c), we consider the specific case of an Fe^{26+} ion moving at $v = 0.7c$, corresponding to a kinetic energy of 20 GeV, as might be realized for various particles in large accelerator facilities [67] and high-intensity plasma wakefield accelerators [68]. Coincidentally, laser acceleration of iron atoms has recently reached nearby energy scales [69]. In this particular case, where the effective fine-structure constant is about 4.9, we see that, at long times, the spectral distribution of emitted photons is highly concentrated around two angle-frequency relations, both substantially different from the conventional Cherenkov relation. These photons are emitted over a short timescale, $t_i \sim 1/\Gamma(z_i)$, of the order of femtoseconds. Interestingly, we find that, for some emission frequencies, the emission angles can be backwards relative to the direction of electron motion, which is impossible in the conventional Cherenkov effect without a negative index of refraction.

Considering the detailed time dynamics of the charge, we find that these multiple poles can translate into a pseudoperiodic decay of the zero-photon state, as can be seen in Fig. 4(b) for a Fe^{26+}. Pushing the effective charge to even larger values, we predict Rabi oscillations of the zero-photon probability, when the imaginary part of one of the poles cancels out (see Ref. [62], Sec. I). These damped Rabi oscillations are similar to those experienced by an atom in strong coupling with a lossy cavity mode [70]. Quantum Rabi oscillations have recently been investigated in ultrastrong-coupling regimes of cavity [71] and circuit QED [72], where a method for treating multiple discrete photonic modes has been proposed. Importantly, unlike bound charge systems that have discrete energy levels, here we work with a charged particle that can take a continuum of energy values. Moreover, the energy scale of free-charge transitions is not limited by the energy levels of AMO systems (can reach the x- or gamma-ray scale and not only visible or IR or below). We should expect new effects that have not been observed in cavity QED, such as the exciting perspective of observing ultrastrong-coupling physics from a single particle in the optical regime. These considerations make the appearance of AMO-physics-inspired phenomena like Rabi oscillation appealing, as no work has ever demonstrated free-charge vacuum Rabi oscillations and related phenomena. Our method could bridge the gap between AMO physics and free-charge physics, allowing us to systematically translate ground-breaking results in AMO to light-matter interactions with free charges.
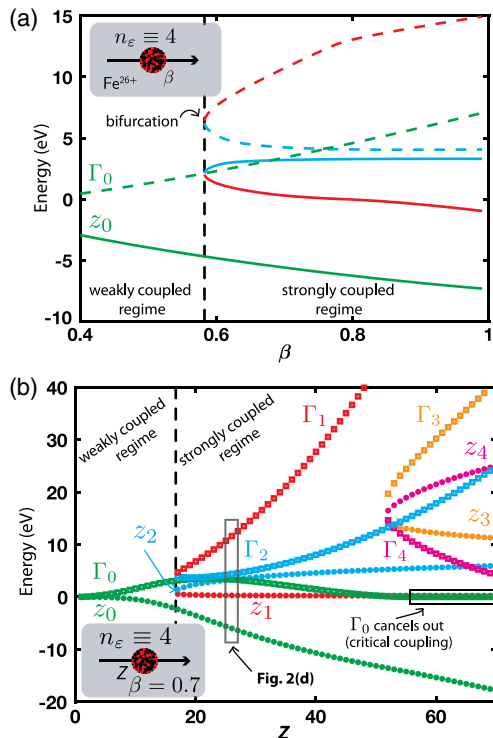
FIG. 5. Cherenkov radiation in the strongly coupled regime: bifurcation process causing abrupt changes in Cherenkov angles. New regimes of behaviors allowed by strong coupling can be explained by studying the poles of the function $f(z)$. (a) Real (solid lines) and imaginary (dashed lines) parts of self-energy $f(z)$ as a function of the reduced speed β of a highly charged ion Fe^{26+}. (b) Real (circles) and imaginary (rectangles) parts of the poles of $f(z)$ as a function of the effective charge number of an ion Z, propagating in a dielectric medium defined by an index window equal to 4. Definitions of weak and strong coupling are consistent with Ref. [10].

To reveal the underlying physics, we analyze the relation between the new nonperturbative Cherenkov dynamics and the pole structure of the regularized self-energy. We show in Fig. 5 how an abrupt change in the pole structure signals a bifurcation process between the conventional Cherenkov dynamics and the strong-coupling physics reported in Fig. 2(c). This transition is characteristic of a bifurcation process, as a small change of a parameter (here, the electron velocity β or the particle charge Z) can result in the emergence of new branches of poles or the cancellation of their imaginary part. Physically, these abrupt changes in the pole structure result, respectively, in new multiple decay modes and Rabi-like oscillations of the decay rate. In order to show the parameter space in which the reported effects are expected to occur, we study the detailed dependence of the poles of $f(z)$ as a function of the ion energy [Fig. 5(a)] and as a function of the ion charge Z altering the effective fine-structure constant α_Z [Fig. 5(b)]. Stronger-coupling regimes can be effectively achieved

either by increasing the velocity of a particle of a given charge Z [Fig. 5(a)] or by increasing the particle's effective charge, at a given speed β [Fig. 5(b)]. In both cases, we denote the emergence of new poles at a given value of β or Z, corresponding to critical coupling. The emerging poles always appear in pairs and split along two branches for larger β or Z. An even larger effective charge results in the emergence of two supplementary poles before canceling the real part of the original pole $\Gamma_0 = 0$ for $Z \geq 56$, which results in the emergence of a Dirac delta function in Eq. (1) and, thus, in the previously mentioned Rabi oscillations.

Cherenkov radiation from highly charged ions in these ranges of energies has been experimentally reported in heavy-ion colliders [25,67]. It is worth mentioning that anomalous Cherenkov radiation in these settings has been observed and attributed, at the time, to superluminal particles—tachyons [26]. The account of the electron relativistic recoil [19,73] was proposed as an explanation for the observation of seemingly superluminal particles. Interestingly, we also predict that the Cherenkov angle of photons radiated by highly charged ions would verify $1/(n_\epsilon \cos \theta_i) > 1$ at some frequencies, which is the behavior expected from superluminal particles [26].

QED interactions are conventionally limited by the size of the fine-structure constant. By increasing the effective fine-structure constant, we explore strong-coupling physics in QED and reveal the presence of bifurcation processes in the Cherenkov effect. The bifurcation is a strong qualitative indicator of new phenomena occurring in these ranges of parameters that may occur at quantitatively different parameters due to other strong-coupling corrections. These findings point to the possibility of studying the physics of strong-coupling field theories like quantum chromodynamics [9], using some of the most commonly studied and relatively accessible effects of QED. The presence of a critical parameter (effective fine-structure constant or electron velocity) with a splitting of the pole branch is reminiscent of a phase transition. However, we should include higher-order processes in the calculation of the nonperturbative self-energy to trust quantitative predictions in these (ultra)strongly coupled settings. Additional corrections occur due to electron-positron creation and annihilation diagrams that dress such high-energy particles in their steady states (corresponding to resummations at all orders in αZ [23], which we can safely neglect when $\alpha Z < 1$). Further corrections also occur due to interactions between the ion and the medium that cannot be described through the macroscopic permittivity of the medium and require a more extensive microscopic description (e.g., bremsstrahlung). For longer times, higher-order diagrams should be taken into account in our calculations; however, it is hard to predict their relative contribution in strongly coupled regimes: For instance, it has recently been predicted that the rate of spontaneous photon emission by an atom in the ultrastrong-coupling regime can actually

decrease as the coupling is increased, suggesting some kind of destructive interference of the bare spontaneous emission diagram with higher-order diagrams that terminate with the emission of a single photon [74]. The smaller decay rate observed in our prediction [Fig. 4(b)] already suggests partially destructive interference between the fundamental Cherenkov diagram and our nonperturbative summation. Higher-order processes and all-order developments in αZ^2 could be integrated in our theory by adequately modifying the coupling between different terms of the resolvent operator.

V. CONCLUSION

In summary, we present a method to regularize time-dependent quantum observables in systems where light and matter interact. Our theory accounts for the nonperturbative self-energy in a time-dependent way. Applied to the Cherenkov effect, we predict readily observable modifications to the conventional theory in weakly coupled regimes and propose a pathway to reveal new physics in strongly coupled regimes that can be effectively achieved with highly charged ions. The observed bifurcation process in the strong-coupling regime originates from the behavior of the self-energy function $f(z)$. Thus, more generally, we should expect to see similar bifurcation processes in any system where strong coupling can be effectively achieved [10]. This observation is especially interesting, since there are Cherenkov analogues in platforms, such as superconducting qubits, where strong-coupling physics is usually observed [34,35], and therefore our predictions could be tested there.

An experiment involving Cherenkov radiation in the strong-coupling regime may also furnish new tests of radiation reaction in dielectric media [75], which is based on the observation that radiation-reaction effects are manifested in the self-energy of the system of the charged particle and the quantized electromagnetic field [76,77]. Further physical understanding of the self-energy can also be provided by adequately transforming the QED Hamiltonian via the Pauli-Fierz transformation, thus clearly exhibiting the interplay between the particle transverse field and mass correction [10].

Other directions to induce stronger-coupling regimes can be investigated by our formalism. Couplings can be enhanced by using systems that display strong light-matter interactions, like photonic cavities, or polaritonic media, which support modes of an effectively high index of refraction. Examples of such polaritonic media are thin metallic films, graphene, and thin polar dielectrics, each of which can potentially support optical modes with an effective mode index of refraction of about 100 [78,79], thus being a promising paradigm for enhanced light-matter interaction [47,65,66]. Another interesting option for achieving free-electron–photon strong coupling is to confine a free electron into a photonic cavity which supports a broadband resonance phase matched to the electron phase velocity, allowing the electron to coherently emit and reabsorb the cavity photons, thus experiencing Rabi oscillations with free electrons.

Additionally, our predictions create new opportunities for the design of ultrafast Cherenkov probes. The theoretical ability to probe short-time dynamics in systems where multiple particles interact pushes towards experimental advances in pump-probe-like experiments or time-dependent electron energy-loss spectroscopy [59,80–82]. More specifically, our findings coincide with the recent development of time-resolved imaging techniques combining electron optics with state-of-the-art spectroscopy [83–86]. We believe these theoretical findings are showing new prospects by which free electrons and other charged particles can provide a platform for the exploration of quantum light-matter interactions and strong-coupling physics.

APPENDIX A: GENERAL TIME-DEPENDENT THEORY OF THE QUANTUM CHERENKOV EFFECT

In this work, we consider the following system: a single electron propagating at speed $v = \beta c$ (momentum $\boldsymbol{p} = m\boldsymbol{v}$), interacting with a continuum of photons with momenta $\boldsymbol{q} = \hbar\boldsymbol{k}$. We consider the following Hilbert space:

$$\mathbb{H} = \mathbb{H}_{el} \otimes \mathbb{H}_{ph}, \tag{A1}$$

where $\mathbb{H}_{el}$ (respectively, $\mathbb{H}_{ph}$) is the Hilbert space describing the quantum states of a single electron (respectively, the full Fock space of photons), defined by its momentum $|\boldsymbol{p}\rangle$ (respectively, by the momentum of every photon $|\boldsymbol{q}, \boldsymbol{q}', \boldsymbol{q}'', \ldots, \boldsymbol{q}^{(N)}, \ldots\rangle$).

We consider the usual QED Hamiltonian to describe the interaction of a spin-1/2 particle with the electromagnetic field [9]:

$$\mathcal{H}_{\text{QED}} = e \int d^3x \bar{\psi} \slashed{A} \psi \tag{A2}$$

$$= e \int d^3x \psi^\dagger \gamma^\mu A_\mu \psi, \tag{A3}$$

where A_μ is the electromagnetic vector potential and $\{\gamma^\mu\}_{\mu \in \{0,1,2,3\}}$ are the Dirac matrices. In this work, we assume that the photon energies are much smaller than the energy of the moving charge, which enables us to neglect spin effects and the charge recoil due to photon emission. Assuming the Coulomb gauge $\nabla \cdot A = 0$ in Eq. (A3), we can show that the coupling Hamiltonian is equal to $V = A \cdot v$, where v is the electron velocity [47].

In the following, we define α as the fine-structure constant

$$\alpha = \frac{e^2}{4\pi\epsilon_0\hbar c}, \tag{A4}$$

and the coupling Hamiltonian V.

Additionally, only the polarization in the (p, q) plane contributes to the coupling. These assumptions allow us to compute the following coupling matrix element:

$$\langle p', q|V|p, 0 \rangle = e\beta \sin\theta \sqrt{\frac{\hbar c^2}{2\Omega\epsilon_0\tilde{\omega}_q}} \int d^3x \frac{e^{-ip' \cdot x}}{\sqrt{\Omega}} e^{-iq \cdot x} \frac{e^{ip \cdot x}}{\sqrt{\Omega}} \tag{A5}$$

$$= ev \sin\theta \sqrt{\frac{\hbar}{2\Omega\epsilon_0\tilde{\omega}_q}} \frac{(2\pi)^3}{\Omega} \delta(-p' - q + p), \tag{A6}$$

where $|p, 0\rangle$ is the quantum state of a single electron propagating with momentum p in the medium, with no photon present. Here, $\tilde{\omega}_q = \frac{1}{2}[\partial/(\partial\omega)](\omega_q^2\varepsilon_\omega) = c^2 q[(\partial q)/(\partial\omega)]$ is the modified normalization factor in a dispersive medium [87] and Ω the normalization volume factor.

1. First-order perturbation theory

We first quickly review the result from the application of Fermi golden rule to this quantum system, to predict the intensity spectrum of Cherenkov radiation. A similar derivation can be found in Ref. [87]. We chose similar notations as in the main text of this article: Ω is the normalization volume factor, $\hbar$ is the reduced Planck constant, ω is the photon energy, and (E_i, p) [respectively, (E_f, p')] are the (energy, momentum) of the initial (respectively, final) states of the electron.

We compute the decay rate of the initial state, given by Fermi's golden rule (FGR):

$$\Gamma_{\text{FGR}} = \frac{2\pi}{\hbar} \int \frac{d^3q}{(2\pi)^3/\Omega} \int \frac{d^3p}{(2\pi)^3/\Omega}$$
$$\times |\langle p', q|V|p, 0 \rangle|^2 \delta[\hbar\omega - (E_i - E_f)]. \tag{A7}$$

Using Eq. (A6), we get the following:

$$\Gamma_{\text{FGR}} = \frac{2\pi}{\hbar} \int \frac{d^3q}{(2\pi)^3/\Omega} \int \frac{d^3p}{(2\pi)^3/\Omega}$$
$$\times \left| ev\sin\theta \sqrt{\frac{\hbar}{2\Omega\epsilon_0\tilde{\omega}_q}} \frac{(2\pi)^3}{\Omega} \delta(-p' - q + p) \right|^2$$
$$\times \delta[\hbar\omega - (E_i - E_f)] \tag{A8}$$

$$= \alpha\beta \int_0^{+\infty} d\omega \left[1 - \left(\frac{1}{n_\omega\beta}\right)^2\right] \Theta\left[\left(\frac{1}{n_\omega\beta}\right)^2 \le 1\right]. \tag{A9}$$

We then find the original Frank-Tamm formula:

$$\frac{d\Gamma_{\text{FGR}}}{d\omega} = \alpha\beta \left[1 - \left(\frac{1}{n_\omega\beta}\right)^2\right] \Theta\left[\left(\frac{1}{n_\omega\beta}\right)^2 \le 1\right]. \tag{A10}$$

where $\Theta[.] = 1$ if the condition between bracket is satisfied, $\Theta[.] = 0$ otherwise, and the subscript ω in n_ω denotes the frequency dependence of the refractive index. We also use the notation n_ε in the future, where $\varepsilon = \hbar\omega$ is the photon energy.

2. Resolvent theory applied to the quantum Cherenkov effect

A comprehensive introduction to the resolvent theory applied to atomic systems in QED can be found in Ref. [10]. The only information we need about the total Hamiltonian $H = H_0 + V$ (where H_0 is the Hamiltonian of the unperturbed system) is

(i) the eigenstates and energies of the unperturbed Hamiltonian H_0 and
(ii) the coupling matrix elements of the perturbation term V, previously used in our derivation of the Fermi golden rule.

The fundamental equation on the resolvent operator G is the following:

$$(z - H_0)G(z) = 1 + VG(z), \tag{A11}$$

where z is a complex energy variable and $G(z)$ is the resolvent operator defined in Ref. [10]. It can be understood as the Fourier transform of the evolution operator $U(t)$. They can be mapped as follows:

$$U(t) = \frac{1}{2\pi i} \oint_{C^+ + C^-} dz\, G(z)e^{-izt/\hbar}, \tag{A12}$$
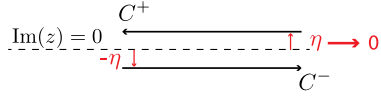
FIG. 6.   Complex integration to Fourier transform the resolvent into the time domain. Complex contour to Fourier invert $G(z)$ to $U(t)$, in the limit $\eta \to 0$. The dashed line in the middle represents the real axis $\text{Im}(z) = 0$.

$$G(z) = \frac{1}{z - H}, \qquad (A13)$$

with $C^+ + C^-$ a complex contour defined as in Fig. 6.

Assuming the system can emit a maximum of one photon, we restrict the photon Hilbert space. It follows that we can get a set of algebraic equations on different matrix elements of the operator $G(z)$, by multiplying Eq. (A11) by adequate bra and ket:

$$(z - E_i)G_0(z) = 1 + \int \frac{d^3\boldsymbol{q}}{(2\pi)^3/\Omega} \frac{d^3\boldsymbol{r}}{(2\pi)^3/\Omega}$$
$$\times V_{(p,0),(r,q)} G_{(r,q),(p,0)}(z), \qquad (A14)$$

$$(z - E_{\boldsymbol{r}} - \hbar\omega_q)G_{(r,q),(p,0)}(z)$$
$$= \int \frac{d^3\boldsymbol{p}}{(2\pi)^3/\Omega} V_{(r,q),(\tilde{p},0)} G_{(\tilde{p},0),(p,0)}(z), \qquad (A15)$$

where, for every operator A, we denote $A_{l,r} = \langle l|A|r \rangle$. The key to solving the dynamics of the system is to identify the self-energy function, which appears in various places along the derivation.

In Ref. [62], Sec. I, we derive another set of fundamental equations on the resolvent operator, by further extending the Hilbert space to more-than-one photon emission. *Let us emphasize that the derivation of the self-energy function (and its regularization) is independent of the approach.*

The simplest way to find the self-energy is by inserting Eq. (A15) in Eq. (A14), and, solving for $G_0(z)$, we get the following expression (momentum conservation is enforced by the coupling Hamiltonian $V_{(r,q),(\tilde{p},0)}$):

$$G_0(z + E_i) = \frac{1}{z - f(z)}, \qquad (A16)$$

where

$$f(z) = \frac{\alpha\beta^2}{2\pi} \int_0^\infty d\varepsilon \int_{-1}^1 du \frac{n_\varepsilon \varepsilon(1 - u^2)}{z - \varepsilon(1 - n_\varepsilon \beta u)}. \qquad (A17)$$

To find $U(t)$, we are interested in values of $f(z)$ arbitrarily close to the real axis, of which we can compute the real and imaginary parts. To get the imaginary part, we use the fact that $\text{Im}[1/(x + i0^+)] = -\pi\delta(x)$:

$$f(z + i0^\pm) = \Delta(z) \mp i\frac{\Gamma(z)}{2}, \qquad (A18)$$

$$\Delta(z) = \frac{\alpha\beta}{2\pi} \int_0^\infty d\varepsilon \left(\frac{2(z - \varepsilon)}{n_\varepsilon \varepsilon\beta} \right)$$
$$+ \left[1 - \left(\frac{z - \varepsilon}{n_\varepsilon \varepsilon\beta} \right)^2 \right] \log\left| \frac{z + \varepsilon(n_\varepsilon\beta - 1)}{z - \varepsilon(n_\varepsilon\beta + 1)} \right|, \qquad (A19)$$

$$\frac{\Gamma(z)}{2} = \frac{\alpha\beta}{2} \int_0^\infty d\varepsilon \left[1 - \left(\frac{\varepsilon - z}{\varepsilon n_\varepsilon\beta} \right)^2 \right] \Theta\left[\left(\frac{\varepsilon - z}{\varepsilon n_\varepsilon\beta} \right)^2 \le 1 \right]. \qquad (A20)$$

We note that $\Gamma(0) = \Gamma_{\text{FGR}}$ and that $\Delta(0)$ matches with the second-order perturbation-theory calculation of the energy shift of $|\boldsymbol{p}, 0\rangle$ due to the electromagnetic coupling. Thus, Eqs. (A18)–(A20) represent a nonperturbative generalization of Cherenkov radiation and the Lamb (radiative) shift of an electron in a medium. These equations are key to developing the results of this paper, and we explore their consequences.

APPENDIX B: REGULARIZATION OF $f(z)$ IN FREQUENCY DOMAIN

This Appendix presents the regularization technique we develop for the purpose of this paper, in order to derive time-dependent regularized observables of the Cherenkov effect. We can readily notice that the real part of $f(z)$ diverges and that it is related to the imaginary part of $f(z)$ being unbounded. Splitting the imaginary part of $f(z)$ into two terms, we observe the following:

$$\frac{\Gamma(z)}{2} = \frac{\Gamma_1(z)}{2} + \frac{\Gamma_2(z)}{2}, \qquad (B1)$$

$$\frac{\Gamma_1(z)}{2} = \frac{\alpha\beta}{2} \int_{n_\varepsilon\beta > 1} d\varepsilon \left[1 - \left(\frac{\varepsilon - z}{\varepsilon n_\varepsilon\beta} \right)^2 \right] \Theta\left[\left(\frac{\varepsilon - z}{\varepsilon n_\varepsilon\beta} \right)^2 \le 1 \right], \qquad (B2)$$

$$\frac{\Gamma_2(z)}{2} = \frac{\alpha\beta}{2} \int_{n_\varepsilon\beta \le 1} d\varepsilon \left[1 - \left(\frac{\varepsilon - z}{\varepsilon n_\varepsilon\beta} \right)^2 \right] \Theta\left[\left(\frac{\varepsilon - z}{\varepsilon n_\varepsilon\beta} \right)^2 \le 1 \right]. \qquad (B3)$$

We can simplify the integration domain of these two functions:

$$\frac{\Gamma_1(z)}{2} = \begin{cases} \frac{\alpha\beta}{2} \int d\varepsilon \left[1 - \left(\frac{\varepsilon - z}{\varepsilon n_\varepsilon\beta} \right)^2 \right] \Theta\left(\varepsilon \ge \frac{z}{1 - n_\varepsilon\beta} \right) & \text{if } z \ge 0, \\ \frac{\alpha\beta}{2} \int d\varepsilon \left[1 - \left(\frac{\varepsilon - z}{\varepsilon n_\varepsilon\beta} \right)^2 \right] \Theta\left(\varepsilon \le \frac{z}{1 + n_\varepsilon\beta} \right) & \text{if } z \le 0, \end{cases}$$
$$\qquad (B4)$$

$$\frac{\Gamma_2(z)}{2} = \begin{cases} \frac{\alpha\beta}{2}\int d\varepsilon \left[1 - \left(\frac{\varepsilon-z}{\varepsilon n_\varepsilon \beta}\right)^2\right]\Theta\left(\frac{z}{1+n_\varepsilon\beta} \le \varepsilon \le \frac{z}{1-n_\varepsilon\beta}\right) & \text{if } z \ge 0, \\ 0 & \text{if } z \le 0. \end{cases}$$

(B5)

(i) When $z \to +\infty$, the Heaviside condition in $\Gamma_1(z)$ forces ε to be very large. In this limit, all materials must have $n_\varepsilon \to 1$ (thus, $n_\varepsilon\beta < 1$), and so the integration domain of $\Gamma_1(z)$ goes to zero. We observe a similar behavior when $z \to -\infty$:

$$\lim_{z \to \pm\infty} \Gamma_1(z, n_\varepsilon) = 0. \qquad (B6)$$

(ii) Because the Heaviside function and the integration domain of Γ_2 have zero intersection when $z < 0$, $\Gamma_2(z, n_\varepsilon)$ is zero for $z < 0$. However, when $z \to +\infty$, the integration domain of $\Gamma_2(z)$ is unbounded, and this integral will diverge:

$$\Gamma_2(z \le 0, n_\varepsilon) = 0, \quad \lim_{z \to +\infty} \Gamma_2(z, n_\varepsilon) = +\infty. \quad (B7)$$

The fact that $\Gamma(z)$ is unbounded results in a misdefinition of $\Delta(z)$, as real and imaginary parts of the analytical function $f(z)$ are related by Kramers-Kronig relations:

$$\Delta(z) = \frac{1}{2\pi}\mathcal{P}\int \frac{\Gamma(z')}{z'-z}dz'. \qquad (B8)$$

A natural way to regularize $f(z)$ in the case of the Cherenkov effect is to subtract the contribution of free space to the integral $n_\varepsilon \equiv 1$, as a free electron propagating in free space at a constant velocity cannot decay and emit a photon. In the following, we define $f(z)$ as the free-space-regularized function:

$$f(z) := f(z) - f(z, n_\varepsilon \equiv 1). \qquad (B9)$$

We find that the regularized self-energy function $f(z)$ is well behaved for realistic refractive indices n_ε. Let us show that with an example, given a linear lossless material, together with the assumption of causality. Under such conditions, it is possible to prove [88] that the index scales like approximately $1 - (1/\varepsilon^2)$ for large ε (here, ε is still the photon energy). We thus get $n_\varepsilon = 1 - (1/\varepsilon^2) + O(1/\varepsilon^2)$ when $\varepsilon \to +\infty$ (it is a direct consequence of the Kramers-Kronig relations [88]). We can thus expand the integrand of the function $f(z) - f(z, n_\varepsilon \equiv 1)$ when $\varepsilon \to +\infty$:

$$\frac{(1-\frac{1}{\varepsilon^2})\varepsilon}{z - \varepsilon[1-(1-\frac{1}{\varepsilon^2})\beta u]} - \frac{\varepsilon}{z - \varepsilon(1-\beta u)} = -\frac{1}{\varepsilon[z - \varepsilon(1-\beta u)]}$$

$$\underset{\varepsilon \to +\infty}{\sim} \frac{1}{\varepsilon^2}, \qquad (B10)$$

which is integrable when $\varepsilon \to +\infty$ (and the integrand is also integrable when $\varepsilon \to 0^+$). Thus, our regularization technique is naturally backed up by fundamental properties of the refractive index n_ε in realistic materials.

We also notice that the renormalized imaginary part $\Gamma(z)/2$ is always positive:

$$\frac{\Gamma(z)}{2} := \int d\varepsilon \left\{ \chi(\varepsilon, n_\varepsilon)\bar{\Theta}\left[\left(\frac{u}{n_\varepsilon}\right)^2\right] - \chi(\varepsilon, 1)\bar{\Theta}[u^2] \right\},$$

(B11)

$$\chi(\varepsilon, n_\varepsilon) = \frac{\alpha\beta}{2}\left[1 - \left(\frac{\varepsilon-z}{\varepsilon n_\varepsilon\beta}\right)^2\right], \qquad (B12)$$

$$u = \frac{\varepsilon-z}{\varepsilon}, \qquad (B13)$$

$$\bar{\Theta}(v) = \mathbb{1}_{[0,1]}(v). \qquad (B14)$$

If $u \le 1$, the integrand is $\chi(\varepsilon, n_\varepsilon) - \chi(\varepsilon, 1) \ge 0$. If $u/n_\varepsilon \le 1$ but $u \ge 1$, the integrand is $\chi(\varepsilon, n_\varepsilon) \ge 0$. Overall, the integrand is positive; thus, $\Gamma(z) \ge 0$ for all z.

APPENDIX C: DERIVATION OF REGULARIZED TIME-DEPENDENT QUANTUM OBSERVABLES

In Ref. [62], Sec. I, we differentiate between two methods, relying on two different assumptions on the Hilbert space in which the quantum state representing our system evolves. The first method is presented in this Appendix. However, in both formulations, the resolvent of the zero-photon state remains the same [given by Eq. (A16)], which results in the same time-dependent evolution of $U_0(t) = \langle p, 0|U(t)|p, 0\rangle$. We show that, by Fourier transforming the resolvent matrix element, one can compute the time evolution of quantum states and relevant observables. In the following, integral limits will often be left implicit.

1. Time-domain derivation of the zero-photon state decay

To solve for the time evolution dynamics of the system, this section first presents the probability of having no photon emission as a function of time.

The value of $f(z)$ above and below the axis are complex conjugated; thus,

$$U_0(t) = \frac{1}{2\pi i}\oint dz\, e^{-izt/\hbar}G_0(z) \qquad (C1)$$

$$= \frac{1}{\pi}e^{-iE_i t/\hbar}\int_{\mathbb{R}} dz\, e^{-izt/\hbar}\frac{\frac{\Gamma(z)}{2}}{[z - \Delta(z)]^2 + (\frac{\Gamma(z)}{2})^2}. \qquad (C2)$$

And the decay probability of the zero-photon state is given by

$$p_0(t) = |U_0(t)|^2. \qquad (C3)$$

We readily notice that the real frequency z_0 verifying $\Delta(z_0) = z_0$ is of particular importance to describe the decay of the zero-photon state. For negligible variations of $f(z)$ around z_0 (flat-continuum approximation), the integrand can be approximated by a Lorentzian peaked at z_0, $\Delta(z_0)$ being an energy shift, while $\Gamma(z_0)/2$ is the decay rate.

$$U_0(t) \approx \exp[-i(E_i + z_0)t/\hbar] \cdot \exp\left[-\frac{1}{2}\Gamma(z_0)t/\hbar\right]. \qquad (C4)$$

Because our expression of the regularized function $f(z)$ matches with first- and second-order perturbation theory, the regular quantum prediction is given by

$$U_0(t) \approx \exp\{-i[E_i + \Delta(0)]t/\hbar\} \cdot \exp\left[-\frac{1}{2}\Gamma(0)t/\hbar\right]. \qquad (C5)$$

When $\Gamma(z_0) = 0$, part of the integrand becomes a Dirac distribution and the zero-photon state only partially decays to a nonzero value $|U_0(+\infty)|^2 = \{1/[1 - (d\Delta(z)/dz)|_{z=z_0}]\}^2$:

$$U_0(t) = e^{-iE_p t/\hbar}\left(\frac{e^{-iz_0 t/\hbar}}{1 - \frac{d\Delta(z)}{dz}\big|_{z=z_0}}\right.$$
$$\left. + \frac{1}{\pi}\int_{z_0+\eta}^{+\infty} dz\, e^{-izt/\hbar}\frac{\Gamma(z)/2}{[z - \Delta(z)]^2 + (\frac{\Gamma(z)}{2})^2}\right). \qquad (C6)$$

In every case, it is obvious that $U_0(0) = 1$.

2. Estimation of z_0 in weakly coupled regime

In practice, we observe that z_0 takes a small negative value for single electrons in optical regimes, which can be seen through the following expansion for small z, in the case of an index constant over an energy range $\Delta\varepsilon$:

$$f(z) \approx \frac{\alpha\beta^2}{2\pi}\left(n\Delta\varepsilon\int\frac{du(1-u^2)}{n\beta u - 1} - z\int\frac{d\varepsilon du(1-u^2)}{\varepsilon(n\beta u - 1)^2}\right). \qquad (C7)$$

Using this expansion around z_0, we get

$$\frac{2\pi}{\alpha\beta^2}z_0 \approx \frac{2\pi}{\alpha\beta^2}[f(z_0) - f(z_0, n_\varepsilon \equiv 1)] \qquad (C8)$$

$$\approx \Delta\varepsilon\int du(1-u^2)\left(\frac{n}{n\beta u - 1} - \frac{1}{\beta u - 1}\right) \qquad (C9)$$

$$-z_0\int d\varepsilon du\,(1-u^2)\left(\frac{n}{\varepsilon(n\beta u - 1)^2} - \frac{1}{\varepsilon(\beta u - 1)^2}\right) \qquad (C10)$$

The second term, proportional to z_0, is of the order of 1, while $[(2\pi)/(\alpha\beta^2)] > 850$ for a single electron; thus, we can safely neglect it. We thus get the following scaling law for z_0:

$$z_0 \sim \frac{\alpha\beta^2}{2\pi}\Delta\varepsilon\left[\int du(1-u^2)\left(\frac{n}{n\beta u - 1} - \frac{1}{\beta u - 1}\right)\right] \qquad (C11)$$

$$\sim -\frac{\alpha\beta^2}{2\pi}\Delta\varepsilon, \qquad (C12)$$

as we can compute the integral term and check that it will take a negative value on the order of -1 when $n\beta \gtrsim 1$ in the optical regime.

3. Spectral angular density of the first emitted photon (closed Hilbert space formulation)

We insert the expression of $G_0(z)$ into Eq. (A15). We use the momentum conservation enforced by the coupling Hamiltonian $V_{(r,q),(\tilde{p},0)}$ to reduce the number of degrees of freedom on $G_{(r,q),(p,0)}(z) = G_{(p-q,q),(p,0)}(z)$. Doing so, the volume factors cancel out, and we get the following expression for $G_{(r,q),(p,0)}(z)$:

$$G_q(z + E_p) := G_{(r,q),(p,0)}(z + E_p)$$
$$= (-ev\sin\theta)\sqrt{\frac{\hbar}{2\Omega\epsilon_0\tilde{\omega}_q}}\frac{1}{z - f(z)}$$
$$\times \frac{1}{z - \hbar\omega_q(1 - \beta n_\omega\cos\theta)}. \qquad (C13)$$

From there, we can readily convert this expression to the time domain and then get the probability of the first emitted photon, by integrating over possible photon momenta q:

$$U_q(t) = \frac{1}{2\pi i}\oint dz\, e^{-izt/\hbar}G_q(z) \qquad (C14)$$

$$= (-ev\sin\theta)\sqrt{\frac{\hbar}{2\Omega\epsilon_0\tilde{\omega}_q}}e^{-iE_p t/\hbar}\frac{1}{\pi}\int dz\, e^{-izt/\hbar}\frac{\frac{\Gamma(z)}{2}}{\{[z - \Delta(z)]^2 + (\frac{\Gamma(z)}{2})^2\}[z - \hbar\omega_q(1 - \beta n_\omega\cos\theta)]}, \qquad (C15)$$

$$p_1(t) = \int \frac{d^3q}{(2\pi)^3/\Omega} |U_q(t)|^2 \tag{C16}$$

$$= \frac{\alpha\beta^2}{2\pi} \int d\varepsilon du \, \varepsilon n_\varepsilon (1-u^2) \left| \frac{1}{\pi} \int dz \, e^{-izt/\hbar} \frac{\frac{\Gamma(z)}{2}}{\{[z-\Delta(z)]^2 + (\frac{\Gamma(z)}{2})^2\}[z-\varepsilon(1-\beta n_\varepsilon u)]} \right|^2 \tag{C17}$$

$$= \int dz' \frac{\Gamma(z')}{2} \left| \frac{1}{\pi} \int dz \, e^{-izt/\hbar} \frac{\frac{\Gamma(z)}{2}}{\{[z-\Delta(z)]^2 + (\frac{\Gamma(z)}{2})^2\}(z-z')} \right|^2. \tag{C18}$$

Equation (C18) gives a frequency-domain expression for $p_1(t)$. We can get another expression for $p_1(t)$, by converting the fundamental Eq. (A15) to the time domain. This conversion is affected through the operation $[1/(2\pi i)] \oint dz$ (still assuming momentum conservation $\mathbf{r} = \mathbf{p} - \mathbf{q}$):

$$-i\hbar e^{-i(E_r+\hbar\omega_q)t/\hbar} \frac{d}{dt} (U_q e^{i(E_r+\hbar\omega_q)t/\hbar}) = (ev\sin\theta) \sqrt{\frac{\hbar}{2\Omega\varepsilon_0\tilde{\omega}_q}} U_0(t), \tag{C19}$$

which gives us, using the expression of $\Gamma(z)$,

$$p_1(t) = \frac{1}{\hbar^2} \int dz \frac{\Gamma(z)}{2} \left| \int_0^t dt' e^{-izt'/\hbar} e^{iE_p t'/\hbar} U_0(t') \right|^2. \tag{C20}$$

In both expressions, we notice that the expression of the imaginary part of $f(z)$ intervenes. We here notice that replacing $\Gamma(z)$ by its regularized form $\Gamma(z) := \Gamma(z) - \Gamma(z, n_\varepsilon \equiv 1)$ is of paramount importance to ensure that the total probability in the Hilbertian space is conserved and equal to 1:

$$p_0(t) + p_1(t) = 1 \quad \forall \, t. \tag{C21}$$

$p_1(t)$ regularization also results in the regularization of the spectral angular density $\{[\partial^2 p_1(t)]/\partial\varepsilon\partial u\}$ using the expression derived from the frequency domain:

$$\frac{\partial^2 p_1(\varepsilon, u, t)}{\partial\varepsilon\partial u} := \frac{\alpha\beta^2}{2\pi} \varepsilon n_\varepsilon (1-u^2) \left| \frac{1}{\pi} \int dz \, e^{-izt/\hbar} \frac{\frac{\Gamma(z)}{2}}{\{[z-\Delta(z)]^2 + (\frac{\Gamma(z)}{2})^2\}[z-\varepsilon(1-\beta n_\varepsilon u)]} \right|^2$$
$$- \frac{\alpha\beta^2}{2\pi} \varepsilon(1-u^2) \left| \frac{1}{\pi} \int dz \, e^{-izt/\hbar} \frac{\frac{\Gamma(z)}{2}}{\{[z-\Delta(z)]^2 + (\frac{\Gamma(z)}{2})^2\}[z-\varepsilon(1-\beta u)]} \right|^2. \tag{C22}$$

And similarly, from the time-domain expression [Eq. (C20)], we get

$$\frac{\partial^2 p_1(t)}{\partial\varepsilon\partial u} := \frac{1}{\hbar^2} \frac{\alpha\beta^2}{2\pi} n_\varepsilon \varepsilon(1-u^2) \left| \int_0^t dt' e^{i\varepsilon(1-n_\varepsilon\beta u)t'/\hbar} e^{-iE_p t'/\hbar} U_0(t') \right|^2 - \frac{1}{\hbar^2} \frac{\alpha\beta^2}{2\pi} \varepsilon(1-u^2) \left| \int_0^t dt' e^{i\varepsilon(1-\beta u)t'/\hbar} e^{-iE_p t'/\hbar} U_0(t') \right|^2. \tag{C23}$$

For convenience, we use the latter expression derived from the time domain in our numerical simulations. In the flat-continuum approximation, we can readily notice that the spectral angular density is enhanced for (ε, u) satisfying

$$\varepsilon(1 - n_\varepsilon \beta u) = z_0 \Leftrightarrow \frac{\varepsilon - z_0}{n_\varepsilon \beta u} = 1, \tag{C24}$$

which coincides with the conventional Cherenkov relation in the case $z_0 = 0$.

This new dispersion relation also allows the existence of backward Cherenkov radiation in this simple setting when $z_0 > 0$ for $\varepsilon < z_0$ [see, for instance, Fig. 2(d)].

APPENDIX D: ADDITIONAL INFORMATION

Additional information can be found in Supplemental Material [62], including a nested Hilbert space formulation, which can take into account several photons, influence of the permittivity function on our predictions, and the generalization of our regularization method to vacuum QED.

———————

[1] W. E. Lamb and R. C. Retherford, *Fine Structure of the Hydrogen Atom by a Microwave Method*, Phys. Rev. **72**, 241 (1947).

[2] S. Tomonaga and J. Robert Oppenheimer, *On Infinite Field Reactions in Quantum Field Theory*, Phys. Rev. **74**, 224 (1948).

[3] H. A. Bethe, *The Electromagnetic Shift of Energy Levels*, Phys. Rev. **72**, 339 (1947).

[4] J. Schwinger, *Quantum Electrodynamics. I. A Covariant Formulation*, Phys. Rev. **74**, 1439 (1948).

[5] R. P. Feynman, *A Relativistic Cut-Off for Classical Electrodynamics*, Phys. Rev. **74**, 939 (1948).

[6] F. J. Dyson, *The Radiation Theories of Tomonaga, Schwinger, and Feynman*, Phys. Rev. **75**, 486 (1949).

[7] P. Kusch and H. M. Foley, *The Magnetic Moment of the Electron*, Phys. Rev. **74**, 250 (1948).

[8] A. Bohr, *On the Hyperfine Structure of Deuterium*, Phys. Rev. **73**, 1109 (1948).

[9] M. Peskin and D. Schroeder, *An Introduction to Quantum Field Theory* (Perseus, Cambridge, MA, 1995).

[10] C. Cohen-Tannoudji, J. Dupont-Roc, and G. Grynberg, *Atom-Photon Interactions: Basic Processes and Applications* (Wiley, Weinheim, 1992).

[11] V. L. Ginzburg, *Applications of Electrodynamics in Theoretical Physics and Astrophysics* (Gordon and Breach, New York, 1989), p. 475.

[12] S. John and T. Quang, *Spontaneous Emission Near the Edge of a Photonic Band Gap*, Phys. Rev. A **50**, 1764 (1994).

[13] R. E. Wagner, Q. Su, and R. Grobe, *Time-Resolved Compton Scattering for a Model Fermion-Boson System*, Phys. Rev. A **82**, 022719 (2010).

[14] L. Garziano, R. Stassi, V. Macrì, A. F. Kockum, S. Savasta, and F. Nori, *Multiphoton Quantum Rabi Oscillations in Ultrastrong Cavity QED*, Phys. Rev. A **92**, 063830 (2015).

[15] P. A. Cherenkov, *Visible Emission of Clean Liquids by Action of γ Radiation*, Dokl. Akad. Nauk SSSR **2**, 451 (1934).

[16] S. I. Vavilov, *On the Possible Causes of Blue γ-Glow of Liquids*, CR Dokl. Akad. Nauk. SSSR. **2**, 8 (1934).

[17] I. Frank and I. Tamm, *Coherent Visible Radiation from Fast Electrons Passing Through Matter*, C.R. Acad. Sci. USSR (1937).

[18] V. L. Ginzburg, *Quantum Theory of Radiation of Electron Uniformly Moving in Medium*, Zh. Eksp. Teor. Fiz. **10**, 589 (1940); J. Phys. USSR **2**, 441 (1940).

[19] A. Sokolow, *Quantum Theory of Cherenkov Effect*, Dokl. Akad. Nauk SSSR (1940).

[20] I. Kaminer, M. Mutzafi, A. Levy, G. Harari, H. H. Sheinfux, S. Skirlo, J. Nemirovsky, J. D. Joannopoulos, M. Segev, and M. Soljacic, *Quantum Cerenkov Radiation: Spectral Cutoffs and the Role of Spin and Orbital Angular Momentum*, Phys. Rev. X **6**, 011006 (2016).

[21] O. Bogdanov, E. Fiks, and Y. Pivovarov, *Angular Distribution of Cherenkov Radiation from Relativistic Heavy Ions Taking into Account Deceleration in the Radiator*, J. Exp. Theor. Phys. **115**, 392 (2012).

[22] V. Koch, A. Majumder, and X. N. Wang, *Cherenkov Radiation from Jets in Heavy-Ion Collisions*, Phys. Rev. Lett. **96**, 172302 (2006).

[23] A. V. Volotka, D. A. Glazov, G. Plunien, and V. M. Shabaev, *Progress in Quantum Electrodynamics Theory of Highly Charged Ions*, Ann. Phys. (Berlin) **525**, 636 (2013).

[24] E. Fiks, O. Bogdanov, and Y. Pivovarov, *New Peculiarities in Angular Distribution of Cherenkov Radiation from Relativistic Heavy Ions Caused by their Stopping in Radiator: Numerical and Theoretical Research* J. Phys. Conf. Ser. **357**, 012002 (2012).

[25] A. S. Vodopianov, Y. I. Ivanshin, V. I. Lobanov, I. I. Tatarinov, A. A. Tyapkin, I. A. Tyapkin, A. I. Zinchenko, V. P. Zrelov, A. A. Bogdanov, V. A. Kaplin, A. I. Karakash, M. F. Runtzo, M. N. Strikhanov, V. M. Biryukov, Y. A. Chesnokov, S. B. Nurushev, J. Ruzicka, P. Chochula, M. Ciljak, and A. Hrmo, *Crystal-Assisted Extraction of Au Ions from RHIC and Application of the Au Beam for the Search of Anomalous Cherenkov Radiation*, Nucl. Instrum. Methods Phys. Res., Sect. B **201**, 266 (2003).

[26] A. S. Vodopianov, V. P. Zrelov, and A. A. Tyapkin, *Analysis of the Anomalous Cherenkov Radiation Obtained in the Relativistic Lead Ion Beam at CERN SPS*, Joint Institute for Nuclear Research Report No. JINR–2-99-2000, 2000.

[27] T. Wulle and S. Herminghaus, *Nonlinear Optics of Bessel Beams*, Phys. Rev. Lett. **70**, 1401 (1993).

[28] C. D'Amico, A. Houard, M. Franco, B. Prade, A. Mysyrowicz, A. Couairon, and V. T. Tikhonchuk, *Conical Forward THz Emission from Femtosecond-Laser-Beam Filamentation in Air*, Phys. Rev. Lett. **98**, 235002 (2007).

[29] S. M. Saltiel, D. N. Neshev, R. Fischer, W. Krolikowski, A. Arie, and Y. S. Kivshar, *Generation of Second-Harmonic Conical Waves via Nonlinear Bragg Diffraction*, Phys. Rev. Lett. **100**, 103902 (2008).

[30] Y. Zhang, Z. D. Gao, Z. Qi, S. N. Zhu, and N. B. Ming, *Nonlinear Čerenkov Radiation in Nonlinear Photonic Crystal Waveguides*, Phys. Rev. Lett. **100**, 163904 (2008).

[31] Y. Sheng, W. Wang, R. Shiloh, V. Roppo, Y. Kong, A. Arie, and W. Krolikowski, *Čerenkov Third-Harmonic Generation in $\chi^{(2)}$ Nonlinear Photonic Crystal*, Appl. Phys. Lett. **98**, 241114 (2011).

[32] K. Vijayraghavan, Y. Jiang, M. Jang, A. Jiang, K. Choutagunta, A. Vizbaras, F. Demmerle, G. Boehm, M. C. Amann, and M. A. Belkin, *Broadly Tunable Terahertz Generation in Mid-Infrared Quantum Cascade Lasers*, Nat. Commun. **4**, 2021 (2013).

[33] M. A. Belkin and F. Capasso, *New Frontiers in Quantum Cascade Lasers: High Performance Room Temperature Terahertz Sources*, Phys. Scr. **90**, 118002 (2015).

[34] A. Wallraff, A. V. Ustinov, V. V. Kurin, I. A. Shereshevsky, and N. K. Vdovicheva, *Whispering Vortices*, Phys. Rev. Lett. **84**, 151 (2000).

[35] J. Pfeiffer, M. Schuster, A. A. Abdumalikov, and A. V. Ustinov, *Observation of Soliton Fusion in a Josephson Array*, Phys. Rev. Lett. **96**, 034103 (2006).

[36] V. Frolov and V. Ginzburg, *Excitation and Radiation of an Accelerated Detector and Anomalous Doppler Effect*, Phys. Lett. A **116**, 423 (1986).

[37] G. Calajó and P. Rabl, *Strong Coupling Between Moving Atoms and Slow-Light Cherenkov Photons*, Phys. Rev. A **95**, 043824 (2017).

[38] X. Shi, X. Lin, I. Kaminer, F. Gao, Z. Yang, J. D. Joannopoulos, M. Soljačić, B. Zhang, and B. Zhang, *Superlight Inverse Doppler Effect*, Nat. Phys. **14**, 1001 (2018).

[39] P. Leboeuf and S. Moulieras, *Superfluid Motion of Light*, Phys. Rev. Lett. **105**, 163904 (2010).

[40] I. Carusotto and G. Rousseaux, *The Čerenkov Effect Revisited: From Swimming Ducks to Zero Modes in Gravitational Analogues*, Analogue Gravity Phenomenology (Springer, Cham, 2013), pp. 109–144.

[41] V. G. Veselago, *The Electrodynamics of Substances with Simultaneously Negative Values of ϵ and μ*, Sov. Phys. Usp. **10**, 509 (1968).

[42] C. Luo, M. Ibanescu, S. G. Johnson, and J. D. Joannopoulos, *Cerenkov Radiation in Photonic Crystals*, Science **299**, 368 (2003).

[43] A. V. Kats, S. Savel'ev, V. A. Yampol'skii, and F. Nori, *Left-Handed Interfaces for Electromagnetic Surface Waves*, Phys. Rev. Lett. **98**, 073901 (2007).

[44] S. Xi, H. Chen, T. Jiang, L. Ran, J. Huangfu, B. I. Wu, J. A. Kong, and M. Chen, *Experimental Verification of Reversed Cherenkov Radiation in Left-Handed Metamaterial*, Phys. Rev. Lett. **103**, 194801 (2009).

[45] F. Liu, L. Xiao, Y. Ye, M. Wang, K. Cui, X. Feng, and W. Zhang, *Integrated Cherenkov Radiation Emitter Eliminating the Electron Velocity Threshold*, Nat. Photonics **11**, 289 (2017).

[46] S. Liu, P. Zhang, W. Liu, S. Gong, R. Zhong, Y. Zhang, and M. Hu, *Surface Polariton Cherenkov Light Radiation Source*, Phys. Rev. Lett. **109**, 153902 (2012).

[47] I. Kaminer, Y. T. Katan, H. Buljan, Y. Shen, O. Ilic, J. J. López, L. J. Wong, J. D. Joannopoulos, and M. Soljačić, *Efficient Plasmonic Emission by the Quantum Cerenkov Effect from Hot Carriers in Graphene*, Nat. Commun. **7**, ncomms11880 (2016).

[48] IceCube Collaboration, *Evidence for High-Energy Extraterrestrial Neutrinos at the IceCube Detector*, Science 2013) 1242856 ,**342**).

[49] T. M. Shaffer, E. C. Pratt, and J. Grimm, *Utilizing the Power of Cerenkov Light with Nanotechnology*, Nat. Nanotechnol. **12**, 106 (2017).

[50] C. Kremers, D. N. Chigrin, and J. Kroha, *Theory of Cherenkov Radiation in Periodic Dielectric Media: Emission Spectrum*, Phys. Rev. A **79**, 013829 (2009).

[51] F. Krausz and M. Ivanov, *Attosecond Physics*, Rev. Mod. Phys. **81**, 163 (2009).

[52] A. H. Zewail, *Femtochemistry: Atomic-Scale Dynamics of the Chemical Bond Using Ultrafast Lasers (Nobel Lecture)*, Angew. Chem. Int. Ed. **39**, 2586 (2000).

[53] A. Kubo, N. Pontius, and H. Petek, *Femtosecond Microscopy of Surface Plasmon Polariton Wave Packet Evolution at the Silver/Vacuum Interface*, Nano Lett. **7**, 470 (2007).

[54] M. Bauer, C. Wiemann, J. Lange, D. Bayer, M. Rohmer, and M. Aeschlimann, *Phase Propagation of Localized Surface Plasmons Probed by Time-Resolved Photoemission Electron Microscopy*, Appl. Phys. A **88**, 473 (2007).

[55] M. I. Stockman, M. F. Kling, U. Kleineberg, and F. Krausz, *Attosecond Nanoplasmonic-Field Microscope*, Nat. Photonics **1**, 539 (2007).

[56] P. Kahl, S. Wall, C. Witt, C. Schneider, D. Bayer, A. Fischer, P. Melchior, M. Horn-von Hoegen, M. Aeschlimann, and F.-J. Meyer zu Heringdorf, *Normal-Incidence Photoemission Electron Microscopy (NI-PEEM) for Imaging Surface Plasmon Polaritons*, Plasmonics **9**, 1401 (2014).

[57] G. Spektor, D. Kilbane, A. K. Mahro, B. Frank, S. Ristok, L. Gal, P. Kahl, D. Podbiel, S. Mathias, H. Giessen, F. J. Meyer Zu Heringdorf, M. Orenstein, and M. Aeschlimann, *Revealing the Subfemtosecond Dynamics of Orbital Angular Momentum in Nanoplasmonic Vortices*, Science **355**, 1187 (2017).

[58] P. Kahl, D. Podbiel, C. Schneider, A. Makris, S. Sindermann, C. Witt, D. Kilbane, M. H.-v. Hoegen, M. Aeschlimann, and F. M. zu Heringdorf, *Direct Observation of Surface Plasmon Polariton Propagation and Interference by Time-Resolved Imaging in Normal-Incidence Two Photon Photoemission Microscopy*, Plasmonics **13**, 239 (2018).

[59] G. M. Vanacore, I. Madan, G. Berruto, K. Wang, E. Pomarico, R. J. Lamb, D. McGrouther, I. Kaminer, B. Barwick, F. J. G. de Abajo, and F. Carbone, *From Attosecond to Zeptosecond Coherent Control of Free-Electron Wave Functions Using Semi-Infinite Light Fields*, Nat. Commun. **9**, 2694 (2018).

[60] R. T. Cox, *Momentum and Energy of Photon and Electron in the Čerenkov Radiation*, Phys. Rev. **66**, 106 (1944).

[61] L. A. Khalfin, *Contribution to the Decay Theory of a Quasi-Stationary State*, Sov. Phys. JETP **6**, 1053 (1958).

[62] See Supplemental Material at http://link.aps.org/supplemental/10.1103/PhysRevX.8.041013 for the nested Hilbert space formulation, which can take into account several photons, the influence of the permittivity function on our predictions, and the generalization of our regularization method to vacuum QED.

[63] A method is proposed in Ref. [62] to take into account diagrams of the successive absorption and reemission of a virtual photon after the emission of the first photon. Taking into account higher-order diagrams (e.g., two-photon emission) requires the computation of the resolvent matrix elements projected on these higher-order states.

[64] K. G. Wilson, *The Renormalization Group: Critical Phenomena and the Kondo Problem*, Rev. Mod. Phys. **47**, 773 (1975).

[65] L. J. Wong, I. Kaminer, O. Ilic, J. D. Joannopoulos, and M. Soljačić, *Towards Graphene Plasmon-Based Free-Electron Infrared to X-ray Sources*, Nat. Photonics **10**, 46 (2016).

[66] N. Rivera, I. Kaminer, B. Zhen, J. D. Joannopoulos, and M. Soljačić, *Shrinking Light to Allow Forbidden Transitions on the Atomic Scale*, Science **353**, 263 (2016).

[67] M. Harrison, T. Ludlam, and S. Ozaki, *RHIC Project Overview*, Nucl. Instrum. Methods Phys. Res., Sect. A **499**, 235 (2003).

[68] I. Blumenfeld, C. E. Clayton, F. J. Decker, M. J. Hogan, C. Huang, R. Ischebeck, R. Iverson, C. Joshi, T. Katsouleas, N. Kirby, W. Lu, K. A. Marsh, W. B. Mori, P. Muggli, E. Oz, R. H. Siemann, D. Walz, and M. Zhou, *Energy Doubling of 42 GeV Electrons in a Metre-Scale Plasma Wakefield Accelerator*, Nature (London) **445,** 741 (2007).

[69] M. Nishiuchi, H. Sakaki, T. Z. Esirkepov, K. Nishio, T. A. Pikuz, A. Y. Faenov, I. Y. Skobelev, R. Orlandi, H. Sako, A. S. Pirozhkov, K. Matsukawa, A. Sagisaka, K. Ogura, M. Kanasaki, H. Kiriyama, Y. Fukuda, H. Koura, M. Kando, T. Yamauchi, Y. Watanabe *et al.*, *Acceleration of Highly Charged GeV Fe Ions from a low-Z Substrate by Intense Femtosecond Laser*, Phys. Plasmas **22,** 033107 (2015).

[70] M. Brune, F. Schmidt-Kaler, A. Maali, J. Dreyer, E. Hagley, J. M. Raimond, and S. Haroche, *Quantum Rabi Oscillation: A Direct Test of Field Quantization in a Cavity*, Phys. Rev. Lett. **76,** 1800 (1996).

[71] O. D. Stefano, R. Stassi, L. Garziano, A. F. Kockum, S. Savasta, and F. Nori, *Feynman-Diagrams Approach to the Quantum Rabi Model for Ultrastrong Cavity QED: Stimulated Emission and Reabsorption of Virtual Particles Dressing a Physical Excitation*, New J. Phys. **19,** 053010 (2017).

[72] M. F. Gely, A. Parra-Rodriguez, D. Bothner, Y. M. Blanter, S. J. Bosman, E. Solano, and G. A. Steele, *Convergence of the Multimode Quantum Rabi Model of Circuit Quantum Electrodynamics*, Phys. Rev. B **95,** 245115 (2017).

[73] G. Afanasiev, M. Lyubchenko, and Y. P. Stepanovsky, *Fine structure of the Vavilov-Cherenkov Radiation*, Proc. R. Soc. A **462,** 689 (2006).

[74] S. De Liberato, *Light-Matter Decoupling in the Deep Strong Coupling Regime: The Breakdown of the Purcell Effect*, Phys. Rev. Lett. **112,** 016401 (2014).

[75] T. N. Wistisen, A. Di Piazza, H. V. Knudsen, and U. I. Uggerhøj, *Experimental Evidence of Quantum Radiation Reaction in Aligned Crystals*, Nat. Commun. **9,** 795 (2018).

[76] J. Dalibard, J. Dupont-Roc, and C. Cohen-Tannoudji, *Vacuum Fluctuations and Radiation Reaction : Identification of Their Respective Contributions*, J. Phys. (Paris) **43,** 1617 (1982).

[77] P. W. Milonni, *The Quantum Vacuum: An Introduction to Quantum Electrodynamics* (Academic, Boston, 1994), p. 522.

[78] D. N. Basov, M. M. Fogler, and F. J. García De Abajo, *Polaritons in van der Waals Materials*, Science **354,** aag1992 (2016).

[79] T. Low, A. Chaves, J. D. Caldwell, A. Kumar, N. X. Fang, P. Avouris, T. F. Heinz, F. Guinea, L. Martin-Moreno, and F. Koppens, *Polaritons in Layered 2D Materials*, Nat. Mater. **16,** 182 (2017).

[80] Y. Morimoto and P. Baum, *Diffraction and Microscopy with Attosecond Electron Pulse Trains*, Nat. Phys. **14,** 252 (2018).

[81] B. Barwick, D. J. Flannigan, and A. H. Zewail, *Photon-Induced Near-Field Electron Microscopy*, Nature (London) **462,** 902 (2009).

[82] A. Feist, K. E. Echternkamp, J. Schauss, S. V. Yalunin, S. Schäfer, and C. Ropers, *Quantum Coherent Optical Phase Modulation in an Ultrafast Transmission Electron Microscope*, Nature (London) **521,** 200 (2015).

[83] F. J. García De Abajo, *Optical Excitations in Electron Microscopy*, Rev. Mod. Phys. **82,** 209 (2010).

[84] L. Piazza, T. T. Lummen, E. Quiñonez, Y. Murooka, B. W. Reed, B. Barwick, and F. Carbone, *Simultaneous Observation of the Quantization and the Interference Pattern of a Plasmonic Near-Field*, Nat. Commun. **6,** 6407 (2015).

[85] T. T. Lummen, R. J. Lamb, G. Berruto, T. Lagrange, L. Dal Negro, F. J. García De Abajo, D. McGrouther, B. Barwick, and F. Carbone, *Imaging and Controlling Plasmonic Interference Fields at Buried Interfaces*, Nat. Commun. **7,** 13156 (2016).

[86] E. Pomarico, I. Madan, G. Berruto, G. M. Vanacore, K. Wang, I. Kaminer, J. García de Abajo, and F. Carbone, *meV Resolution in Laser-Assisted Energy-Filtered Transmission Electron Microscopy*, ACS Photonics **5,** 759 (2017).

[87] E. Harris, *A Pedestrian Approach to Quantum Field Theory* (Dover, New York, 2014).

[88] L. Davidovich, L. D. Landau, E. M. Lifshitz, and L. P. Pitaevskii, *Electrodynamics of Continuous Media* (Pergamon, New York, 1984), p. 460.